Supplementary Information Titles

Journal: Nature Medicine

Article Title:	Combination inhibition of PI3K and mTORC1 yields durable remissions in orthotopic patient-derived xenografts of HER2-positive breast cancer brain metastases
Corresponding Author:	J.J.Z. (jean_zhao@dfci.harvard.edu), K.L.L. (keith_ligon@dfci.harvard.edu), N.U.L. (nancy_lin@dfci.harvard.edu), or E.P.W. (eric_winer@dfci.harvard.edu).

Supplementary Item & Number	Title or Caption
Supplementary Figure 1	Kaplan-Meier survival of mice bearing DF-BM354 and DF-BM355 primary grafts (P0)
Supplementary Figure 2	Selective response of HER2-positive BCBM PDX DF-BM355 to the combination of BKM120/RAD001
Supplementary Figure 3	The combination of BKM120/MEK162 has little effect on DF-BM354 tumor growth
Supplementary Figure 4	The combination of BKM120/JQ1 has little effect on DF-BM355 tumor growth
Supplementary Figure 5	Differential responses of HER2-positive BCBM PDXs to the combination of BKM120/RAD001
Supplementary Figure 6	Genome-wide DNA CNVs in HER2-positive BCBM PDXs analyzed by WES
Supplementary Figure 7	Conservation of genetic alternations after the transfer of tissue from patient to mouse
Supplementary Table 1	Summary of histological and immunophenotypic analysis of five HER2-positive BCBM PDX models
Supplementary Table 2	The treatment histories of HER2-positive BCBM patients who contributed their specimens to the derivation of PDXs
Supplementary Table 3	A list of mutations in DNA repair genes found in DF-BM507 and DF-BM590
Supplementary Table 4	A list of mutations in DNA repair genes found in patient brain metastatic tumors of DF-BM507 and DF-BM590
Supplementary methods	

Supplemental Figures

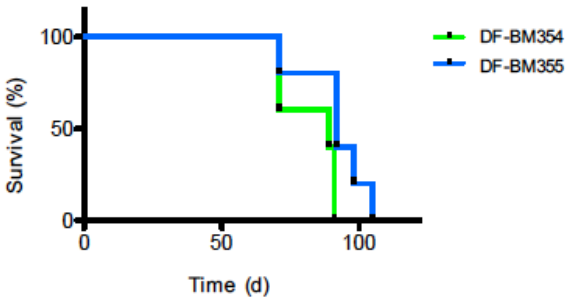

Supplementary Figure 1: Kaplan-Meier survival of mice bearing DF-BM354 and DF-BM355 primary grafts (P0). Fresh human HER2-positive breast cancer brain metastases DF-BM354 and DF-BM355 were dissociated and intracranially injected into female SCID mice (*n* = 5 mice per group).

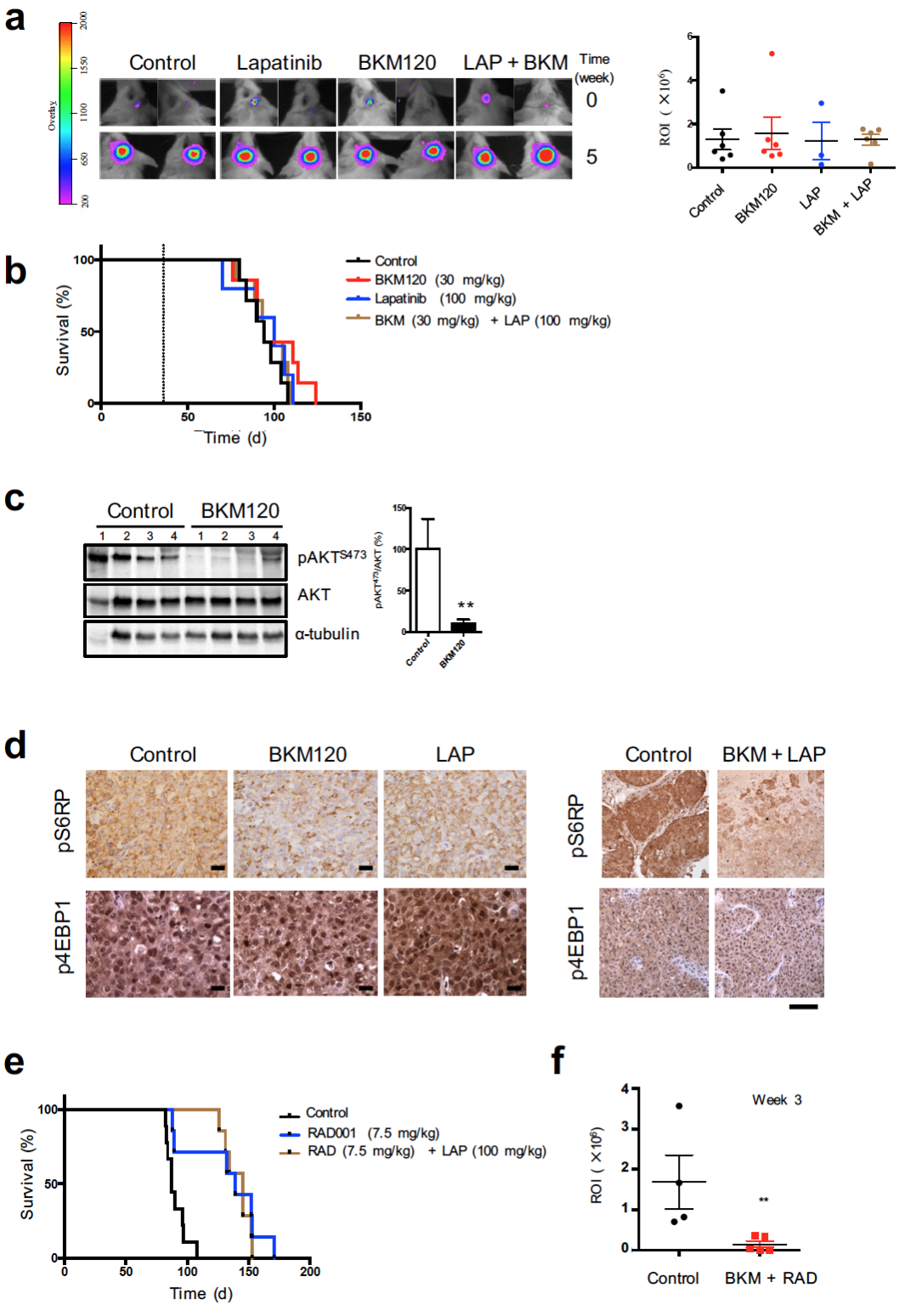

Supplementary Figure 2: Selective response of HER2-positive PDX DF-BM355 to the combination of BKM120/RAD001. (**a**) Left, representative bioluminescence imaging analysis

of mice bearing DF-BM355 tumors at week 0 and week 5 after treatment with vehicle control (n = 6), Lapatinib (n = 3), BKM120 (n = 6), or combined Lapatinib with BKM120 (n = 6). Right, quantification of bioluminescence for the brain region of interest (ROI) for the indicated treatment. mean ± s.d., n = 3–6 female SCID mice per group. (**b**) Kaplan-Meier survival of mice bearing DF-BM355 treated with vehicle control (black, n = 7), BKM120 (red, PO, 30 mg/kg, QD, n = 7), Lapatinib (blue, PO, 100 mg/kg, n = 5), BKM120 + Lapatinib (BKM + LAP, brown, n = 7). (**c**) Western blot analysis of lysates from vehicle-treated or BKM120-treated DF-BM355 *in vivo*. Bar graph represents mean ± s.d. of western blot quantification of $pAKT^{S473}$/AKT (n = 4, $^{**}P < 0.01$, Student's t-test). (**d)** IHC analyses of pS6RP and p4EBP on DF-BM355 tumors with vehicle, BKM120 (PO 30 mg/kg, QD), LAP (PO 100 mg/kg, QD) or BKM120 + LAP. Scale bars = 25 μm (left) and 100 μm (right). (**e**) Kaplan-Meier survival of mice bearing DF-BM355 treated with vehicle control (black, n = 9), RAD001 (blue, PO 7.5 mg/kg, QD, n = 7), or Lapatinib + RAD001 (brown, n = 9). (**f**) Quantification of bioluminescence for the brain region of interest (ROI) for the indicated treatment. mean ± s.d., n = 4–5 female SCID mice per group, $^{**}P < 0.01$.

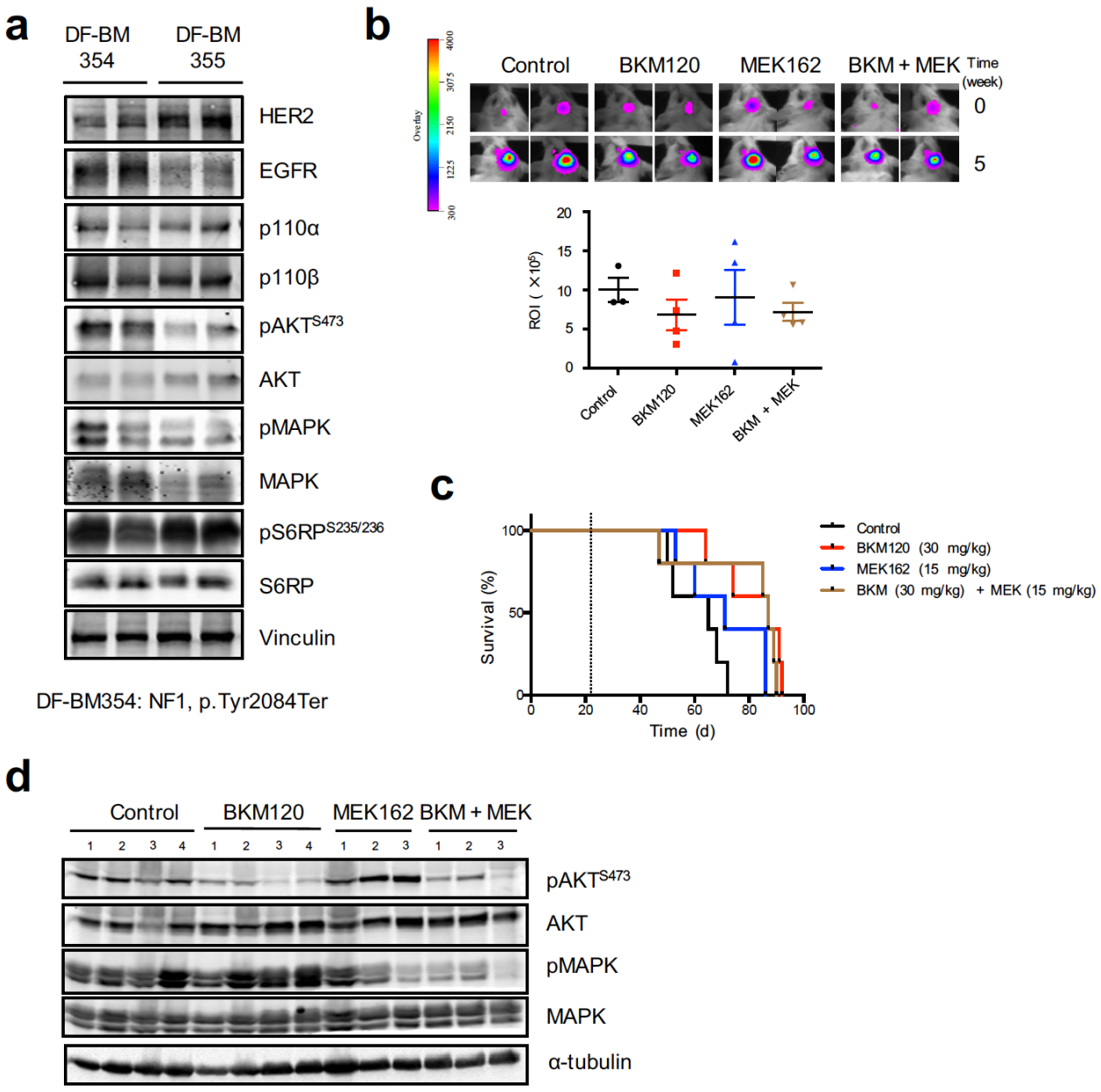

Supplementary Figure 3: The combination of BKM120/MEK162 has little effect on DF-BM354 tumor growth. (**a**) Western blot analysis of PI3K/mTOR/MAPK signaling in DF-BM354 compared to DF-BM355. (**b**) Top, representative bioluminescence imaging analysis of DF-BM354 before (week 0) and after (week 5) treatment with indicated compounds. *n* = 3–4. Bottom, quantification of bioluminescence for the brain region of interest (ROI) for the indicated

treatment. (**c**) Kaplan-Meier survival of mice treated with BKM120 (red, PO, 30 mg/kg, QD), MEK162 (blue, PO, 15 mg/kg), BKM120 + MEK162 (brown), or vehicle control (black). $n = 5$. (**d**) Western blot analysis of lysates from DF-BM354 tumors treated with vehicle, BKM120, MEK162, or BKM120/MEK162 *in vivo*.

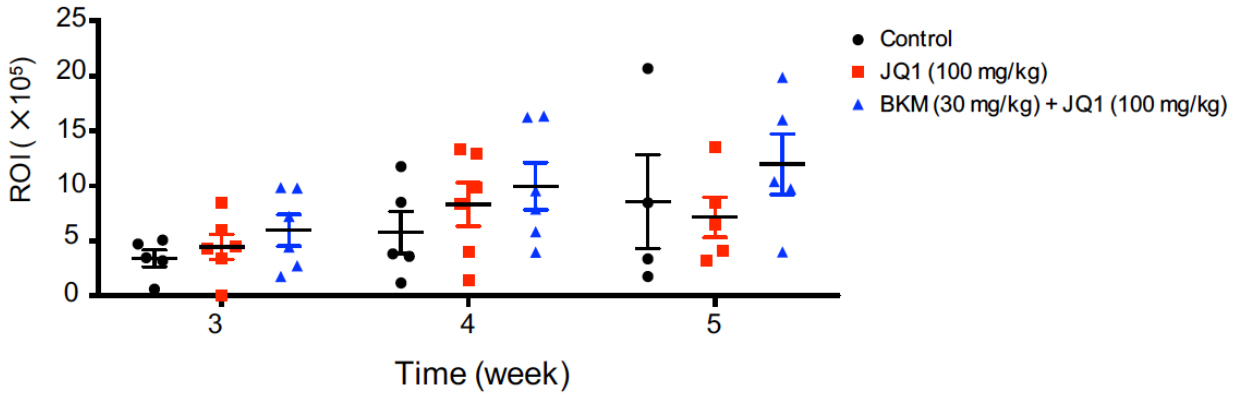

Supplementary Figure 4: The combination of BKM120/JQ1 has little effect on DF-BM355 tumor growth. Mice bearing DF-BM355 tumors were treated with JQ1 (red, IP, 100 mg/kg, QD), JQ1 + BKM120 (blue), or vehicle control (black). The tumor burden is represented by quantification of bioluminescence induction for the brain region of interest (ROI). *n* = 5–6.

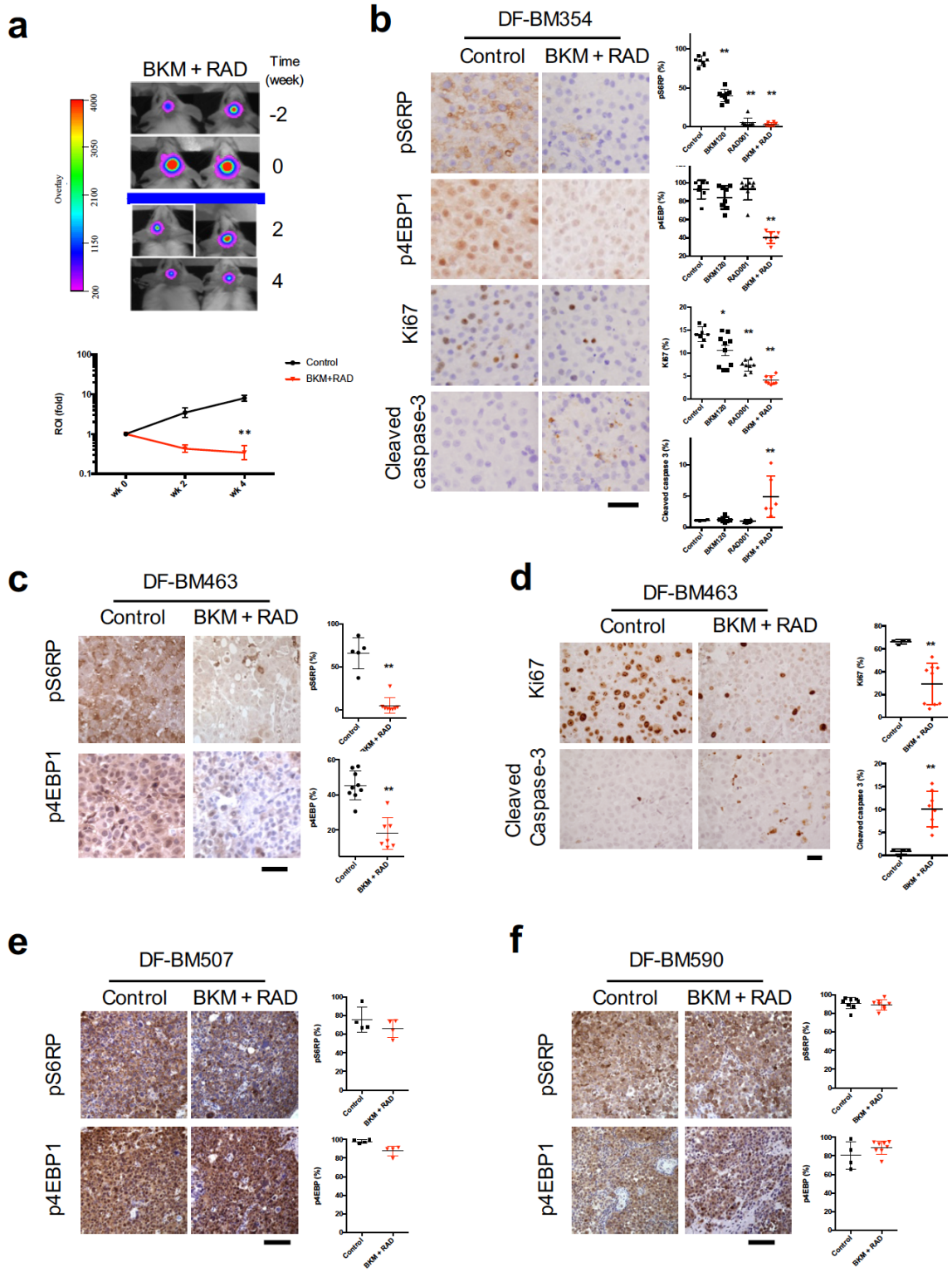

Supplementary Figure 5: Differential responses of HER2-positive BCBM PDXs to the combination of BKM120/RAD001. (**a**) Representative bioluminescence imaging analysis of

DF-BM354 before (wk -2 and wk 0) and after (wk 2 and wk 4) treatment with combined BKM120 and RAD001 (BKM120, PO 30 mg/kg, QD; RAD001, PO 7.5mg/kg, QD) (top) and quantification of bioluminescence for the brain region of interest (ROI) for the indicated treatment (bottom). (mean ± s.d., $n = 3–5$, $^{**}P < 0.01$, Student's *t*-test). (**b**) IHC analyses of DF-BM354 tumors harvested from tumor bearing mice treated for 4 days with vehicle or BKM120 + RAD001 with indicated antibodies (scale bars = 25 μm). Graphs represent mean ± s.d. ($^{*}P < 0.05$, $^{**}P < 0.01$, one-way ANOVA followed by Dunnett's test). (**c, d**) IHC analyses of DF-BM463 tumors harvested from tumor bearing mice treated for 4 days with vehicle or BKM120 + RAD001 with indicated antibodies (**c**, scale bar = 50 μm; **d**, scale bar = 25 μm). Graphs represent mean ± s.d. ($^{**}P < 0.01$, Student's *t*-test). (**e**) IHC analyses of DF-BM507 tumors harvested from tumor bearing mice treated 4 days with vehicle or BKM120 + RAD001 with indicated antibodies (scale bars = 100 μm). Graphs represent mean ± s.d.. (**f**) IHC analyses of DF-BM590 tumors treated with vehicle or BKM120 + RAD001 with indicated antibodies (scale bars = 100 μm). Graphs represent mean ± s.d..

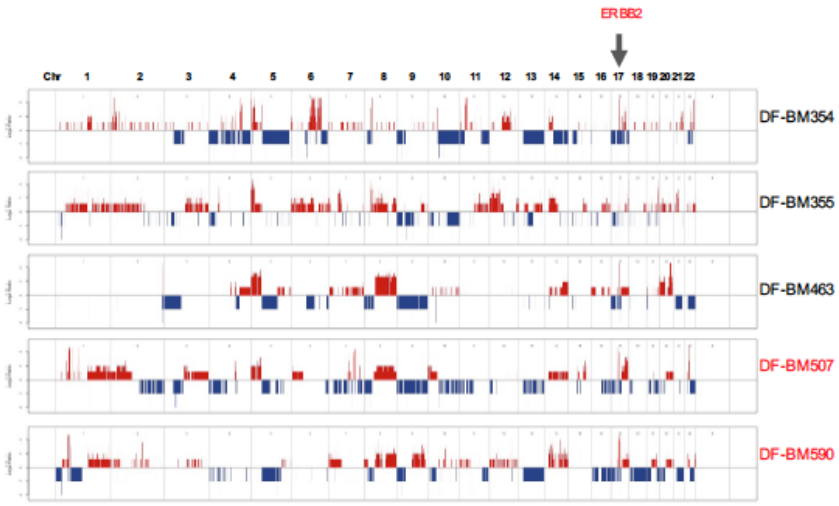

Supplementary Figure 6: Genome-wide DNA CNVs in HER2-positive BCBM PDXs analyzed by WES.

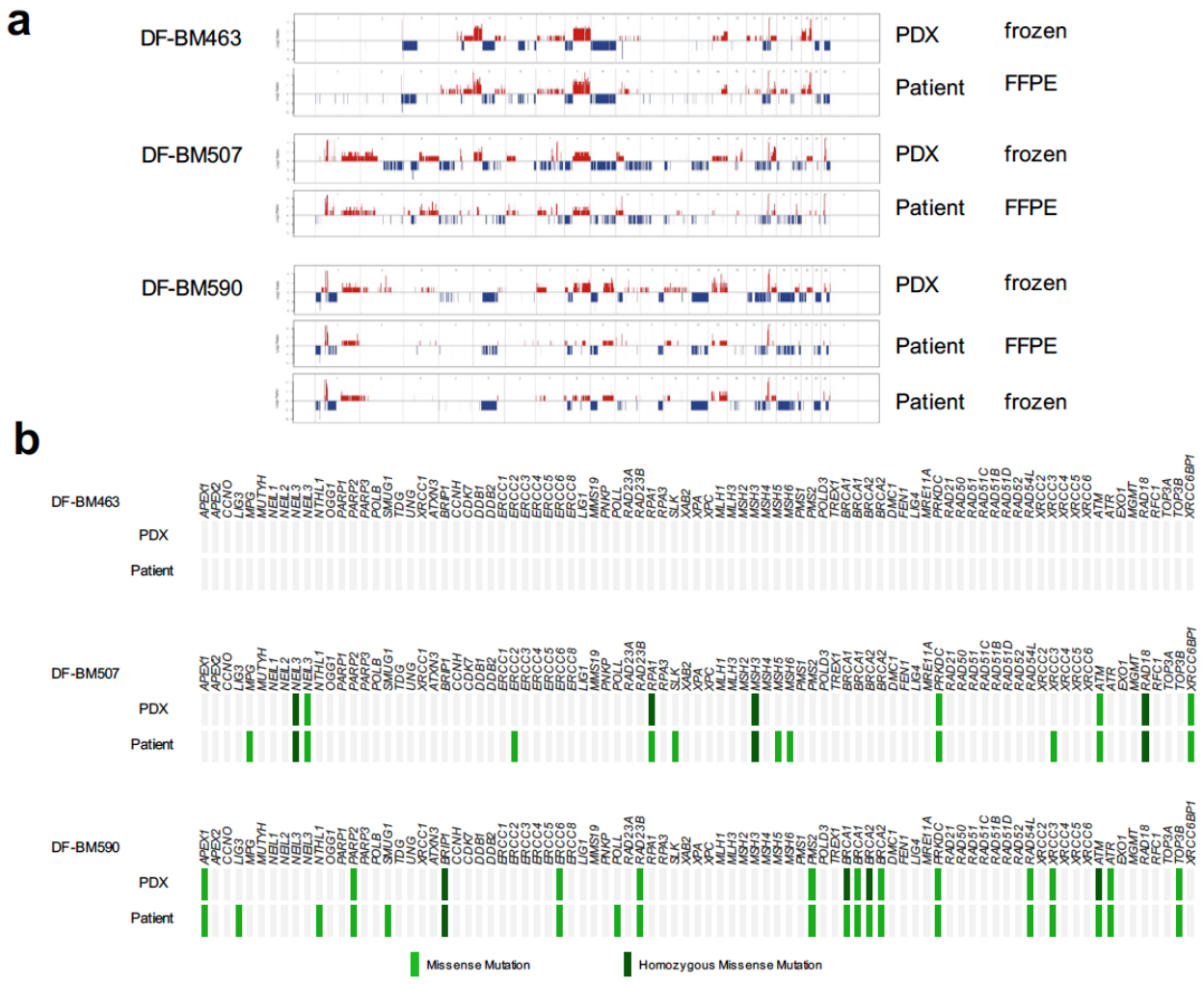

Supplementary Figure 7: Conservation of genetic alternations after the transfer of tissue from patient to mouse. (**a**) Patterns of genome-wide DNA copy number variations in DF-BM463, DF-BM507 and DF-BM590 PDXs and their matched patient tumors. (**b**) Mutational profiling of a panel of DNA repair genes in DF-BM463, DF-BM507 and DF-BM590 PDXs and their matched patient tumors.

Supplementary Table 1: Summary of histological and immunophenotypic analysis of five HER2-positive BCBM PDX models

DF-BM#	HER2	ER	PR	PTEN
354	+++	-	-	-
355	+++	+	-	-
463	+++	+	-	-
507	+++	-	-	-
590	+++	-	-	-

Supplementary Table 2: The treatment histories of HER2-positive BCBM patients who contributed their specimens to the derivation of PDXs

	Target therapy	Chemotherapy	Hormone therapy	Radiation
DF-BM354	trastuzumab	vinorelbine	none	2 separate episodes of stereotactic radiation to donor metastasis
DF-BM355	trastuzumab	taxol, capecitabine	none	whole brain radiotherapy, stereotactic radiation
DF-BM463	trastuzumab	doxorubicin, cyclophosphamide, paclitaxel	tamoxifen	none
DF-BM507	trastuzumab, lapatinib, neratinib	doxorubicin, cyclophosphamide, paclitaxel, vinorelbine, capecitabine	none	Whole Brain Radiotherapy
DF-BM590	trastuzumab, lapatinib, neratinib	doxorubicin, cyclophosphamide, paclitaxel, carboplatin, capecitabine	none	Whole Brain Radiotherapy

Supplementary Table 3: A list of mutations in DNA repair genes found in DF-BM507 and DF-BM590

sample	gene	locus	type	ref	length	genotype	coverage	allele_coverage	transcript	location	function.	codon	protein	coding	normalizedAlt	cosmic	blood_genotype	blood_coverage	blood_allele_coverage
DF-BM507	ATM	chr11:108175462	SNV	G	1	G/A	99	68,31	NM_000051.3	exonic	missense	AAT	p.Asp1853Asn	c.5557G>A	A	41596	G/G	44	44,0
DF-BM507	XRCC6BP1	chr12:58335626	SNV	A	1	A/T	64	36,28	NM_033276.2	exonic	missense	TGC	p.Ser48Cys	c.142A>T	T	431609	A/A	86	86,0
DF-BM507	NEIL3	chr4:178274835	SNV	A	1	C/C	78	2,76	NM_018248.2	exonic	missense	CAC	p.Gln471His	c.1413A>C	C	1428751:1131168	A/A	85	85,0
DF-BM507	MSH3	chr5:80168937	SNV	G	1	A/A	26	0,26	NM_002439.4	exonic	missense	ACA	p.Ala1045Thr	c.3133G>A	A		G/G	91	91,0
DF-BM507	NEIL3	chr4:178274750	SNV	C	1	T/T	76	0,76	NM_018248.2	exonic	missense	CTA	p.Pro443Leu	c.1328C>T	T		C/C	93	93,0
DF-BM507	PRKDC	chr8:48841708	SNV	G	1	G/A	152	46,106	NM_006904.6	exonic	missense	TCT	p.Pro695Ser	c.2083C>T	A		./.	13	13,0
DF-BM507	RAD18	chr3:8955389	SNV	C	1	T/T	70	0,70	NM_020165.3	exonic	missense	CAA	p.Arg302Gln	c.905G>A	T		./.	6	5,1
DF-BM507	RPA1	chr17:1782952	SNV	A	1	G/G	72	0,72	NM_002945.3	exonic	missense	GCA	p.Thr351Ala	c.1051A>G	G		A/A	192	192,0
DF-BM590	ATM	chr11:108175462	SNV	G	1	A/A	70	0,70	NM_000051.3	exonic	missense	AAT	p.Asp1853Asn	c.5557G>A	A	41596	./.	16	16,0
DF-BM590	BRCA1	chr17:41244000	SNV	T	1	C/C	80	4,76	NM_007300.3	exonic	missense	AGA	p.Lys1183Arg	c.3548A>G	C	148277	T/T	63	63,0
DF-BM590	BRCA1	chr17:41244936	SNV	G	1	A/A	36	0,36	NM_007300.3	exonic	missense	CTG	p.Pro871Leu	c.2612C>T	A	148278	./.	18	18,0
DF-BM590	ATR	chr3:142178144	SNV	C	1	C/T	71	37,34	NM_001184.3	exonic	missense	CAA	p.Arg2425Gln	c.7274G>A	T	149485	./.	4	4,0
DF-BM590	PMS2	chr7:6026942	SNV	G	1	G/T	293	135,158	NM_000535.5	exonic	missense	AAG	p.Thr485Lys	c.1454C>A	T	150232	G/G	83	82,0
DF-BM590	APEX1|TMEM55B	chr14:20925154	SNV	T	1	T/G	158	83,75	NM_001244249.1|NM_001100814.2	exonic|downstream	missense|	GAG|	p.Asp148Glu|	c.444T>G|	G|		T/T	66	66,0
DF-BM590	BRCA1	chr17:41223094	SNV	T	1	C/C	81	6,75	NM_007300.3	exonic	missense	GGT	p.Ser1634Gly	c.4900A>G	C		T/T	29	29,0
DF-BM590	BRCA1	chr17:41244435	SNV	T	1	C/C	26	2,24	NM_007300.3	exonic	missense	GGA	p.Glu1038Gly	c.3113A>G	C		T/T	33	33,0
DF-BM590	BRCA2	chr13:32906480	SNV	A	1	C/C	73	2,71	NM_000059.3	exonic	missense	CAT	p.Asn289His	c.865A>C	C		A/A	81	81,0
DF-BM590	BRCA2	chr13:32911463	SNV	A	1	G/G	51	0,51	NM_000059.3	exonic	missense	GAC	p.Asn991Asp	c.2971A>G	G		A/A	79	79,0
DF-BM590	BRIP1	chr17:59763347	SNV	A	1	G/G	161	0,161	NM_032043.2	exonic	missense	CCA	p.Ser919Pro	c.2755T>C	G		A/A	44	44,0
DF-BM590	ERCC6	chr10:50680422	SNV	C	1	C/T	139	72,67	NM_000124.3	exonic	missense	CAA	p.Arg975Gln	c.2924G>A	T		./.	24	24,0
DF-BM590	ERCC6|PGBD3|ERCC6-PGBD3|ERCC6-PGBD3	chr10:50732139	SNV	C	1	C/T	41	18,23	NM_000124.3|NM_170753.3|NM_001277058.1|NM_001277059.1	exonic|utr_5|exonic|exonic	missense||missense|missense	GAT||GAT|GAT	p.Gly446Asp||p.Gly446Asp|p.Gly446Asp	c.1337G>A||c.1337G>A||c.1337G>A	T||T|T		C/C	56	57,0
DF-BM590	PARP2	chr14:20819232	SNV	G	1	G/A	173	78,95	NM_005484.3	exonic	missense	ATG	p.Val163Met	c.487G>A	A		G/G	86	86,0
DF-BM590	PRKDC	chr8:48710955	SNV	A	1	A/G	353	124,229	NM_006904.6	exonic	missense	ACT	p.Ile3433Thr	c.10300T>C	G		A/A	69	69,0
DF-BM590	RAD23B	chr9:110084328	SNV	C	1	C/T	393	78,315	NM_002874.4	exonic	missense	GTT	p.Ala249Val	c.746C>T	T		./.	15	15,0
DF-BM590	RAD54L	chr1:46725684	SNV	G	1	G/A	88	61,27	NM_001142548.1	exonic	missense	CAG	p.Arg107Gln	c.320G>A	A		G/G	75	76,0
DF-BM590	TOP3B	chr22:22318364	SNV	G	1	G/A	99	41,58	NM_003935.4	exonic	missense	TGG	p.Arg379Trp	c.1135C>T	A		G/G	48	48,0
DF-BM590	XRCC3	chr14:104169515	SNV	C	1	C/A	301	156,145	NM_001100118.1	exonic	missense	TAT	p.Asp186Tyr	c.556G>T	A		C/C	110	111,0

yellow highlight for COSMIC mutation

Supplementary Table 4: A list of mutations in DNA repair genes found in patient brain metastatic tumors of DF-BM507 and DF-BM590

patient	gene	locus	type	ref	length	genotype	coverage	allele_coverage	transcript	location	function.	codon	protein	coding	normalizedAlt	cosmic	blood_genotype.1	blood_coverage	blood_allele_coverage
MN507	ATM	chr11:108175462	SNV	G	1	G/A	140	97,43	NM_000051.3	exonic	missense	AAT	p.Asp1853Asn	c.5557G>A	A	41596	G/G	44	44,0
MN507	XRCC6BP1	chr12:58335626	SNV	A	1	A/T	494	350,144	NM_033276.2	exonic	missense	TGC	p.Ser48Cys	c.142A>T	T	431609	A/A	85	85,0
MN507	NEIL3	chr4:178274835	SNV	A	1	C/C	62	1,61	NM_018248.2	exonic	missense	CAC	p.Gln471His	c.1413A>C	C	1131168:1428751	A/A	86	86,0
MN507	KLC3|ERCC2	chr19:45854919	SNV	T	1	T/G	132	69,63	NM_177417.2|NM_000400.3	downstream|exonic	|missense	|CAG	|p.Lys751Gln	|c.2251A>C	|G		T/T	93	92,0
MN507	MPG|NPRL3	chr16:135414	SNV	G	1	G/A	130	60,70	NM_001015052.2|NM_001077350.2	exonic|downstream	missense|	ATC|	p.Val174Ile|	c.520G>A|	A|		G/G	47	47,0
MN507	MSH3	chr5:80168937	SNV	G	1	A/A	87	1,86	NM_002439.4	exonic	missense	ACA	p.Ala1045Thr	c.3133G>A	A		G/G	93	93,0
MN507	MSH5|MSH5-SAPCD1	chr6:31708328	SNV	C	1	C/T	58	19,39	NM_172165.3|NR_037846.1	exonic|exonic_nc	missense|	TCA|	p.Pro29Ser|	c.85C>T|	T|		C/C	27	27,0
MN507	MSH6	chr2:48026045	SNV	G	1	G/A	166	144,22	NM_000179.2	exonic	missense	GAC	p.Gly308Asp	c.923G>A	A		G/G	106	106,0
MN507	NEIL3	chr4:178262784	SNV	A	1	A/G	138	101,37	NM_018248.2	exonic	missense	CGT	p.His286Arg	c.857A>G	G		A/A	100	101,0
MN507	NEIL3	chr4:178274750	SNV	C	1	T/T	73	1,72	NM_018248.2	exonic	missense	CTA	p.Pro443Leu	c.1328C>T	T		C/C	93	93,0
MN507	PRKDC	chr8:48841708	SNV	G	1	G/A	174	31,143	NM_006904.6	exonic	missense	TCT	p.Pro695Ser	c.2083C>T	A		./.	13	13,0
MN507	RAD18	chr3:8955389	SNV	C	1	T/T	34	1,33	NM_020165.3	exonic	missense	CAA	p.Arg302Gln	c.905G>A	T		./.	6	5,1
MN507	RPA1	chr17:1782952	SNV	A	1	A/G	146	27,119	NM_002945.3	exonic	missense	GCA	p.Thr351Ala	c.1051A>G	G		A/A	190	190,0
MN507	SLK	chr10:105762591	SNV	G	1	G/A	69	45,24	NM_014720.2	exonic	missense	TAT	p.Cys552Tyr	c.1655G>A	A		./.	23	23,0
MN507	SLK	chr10:105762909	SNV	C	1	C/G	95	58,37	NM_014720.2	exonic	missense	GGT	p.Ala658Gly	c.1973C>G	G		./.	11	11,0
MN507	XRCC3	chr14:104169599	SNV	G	1	G/A	177	156,21	NM_001100118.1	exonic	nonsense	TAG	p.Gln158Ter	c.472C>T	A		G/G	279	279,0
MN590	ATM	chr11:108175462	SNV	G	1	G/A	83	12,71	NM_000051.3	exonic	missense	AAT	p.Asp1853Asn	c.5557G>A	A	41596	./.	17	17,0
MN590	BRCA1	chr17:41244000	SNV	T	1	T/C	94	10,84	NM_007300.3	exonic	missense	AGA	p.Lys1183Arg	c.3548A>G	C	148277	T/T	63	63,0
MN590	BRCA1	chr17:41244936	SNV	G	1	A/A	80	3,77	NM_007300.3	exonic	missense	CTG	p.Pro871Leu	c.2612C>T	A	148278	./.	18	18,0
MN590	ATR	chr3:142178144	SNV	C	1	C/T	84	40,44	NM_001184.3	exonic	missense	CAA	p.Arg2425Gln	c.7274G>A	T	149485	./.	4	4,0
MN590	PMS2	chr7:6026942	SNV	G	1	G/T	299	139,160	NM_000535.5	exonic	missense	AAG	p.Thr485Lys	c.1454C>A	T	150232	G/G	78	79,0
MN590	APEX1|TMEM55B	chr14:20925154	SNV	T	1	T/G	238	95,143	NM_001244249.1|NM_001100814.2	exonic|downstream	missense|	GAG|	p.Asp148Glu|	c.444T>G|	G|		T/T	65	65,0
MN590	BRCA1	chr17:41223094	SNV	T	1	T/C	134	50,84	NM_007300.3	exonic	missense	GGT	p.Ser1634Gly	c.4900A>G	C		T/T	30	30,0
MN590	BRCA1	chr17:41244435	SNV	T	1	T/C	87	19,68	NM_007300.3	exonic	missense	GGA	p.Glu1038Gly	c.3113A>G	C		T/T	34	34,0
MN590	BRCA2	chr13:32906480	SNV	A	1	A/C	52	6,46	NM_000059.3	exonic	missense	CAT	p.Asn289His	c.865A>C	C		A/A	87	87,0
MN590	BRCA2	chr13:32911463	SNV	A	1	A/G	72	15,57	NM_000059.3	exonic	missense	GAC	p.Asn991Asp	c.2971A>G	G		A/A	76	76,0
MN590	BRIP1	chr17:59763347	SNV	A	1	G/G	113	0,113	NM_032043.2	exonic	missense	CCA	p.Ser919Pro	c.2755T>C	G		A/A	46	46,0
MN590	ERCC6	chr10:50680422	SNV	C	1	C/T	170	84,86	NM_000124.3	exonic	missense	CAA	p.Arg975Gln	c.2924G>A	T		./.	23	23,0
MN590	ERCC6|PGBD3|ERCC6-PGBD3|ERCC6-PGBD3	chr10:50732139	SNV	C	1	C/T	46	21,25	NM_000124.3|NM_170753.3|NM_001277058.1|NM_001277059.1	exonic|utr_5|exonic|exonic	missense||missense|missense	GAT||GAT|GAT	p.Gly446Asp||p.Gly446Asp||p.Gly446Asp	c.1337G>A||c.1337G>A||c.1337G>A	T||T|T		C/C	55	57,0
MN590	LIG3	chr17:33329109	SNV	C	1	C/T	104	72,32	NM_013975.3	exonic	missense	TTC	p.Ser887Phe	c.2660C>T	T		C/C	65	65,0
MN590	NTHL1	chr16:2094653	SNV	A	1	A/G	53	26,25	NM_002528.5	exonic	missense	ACC	p.Ile176Thr	c.527T>C	G		A/A	60	60,0
MN590	PARP2	chr14:20819232	SNV	G	1	G/A	121	35,86	NM_005484.3	exonic	missense	ATG	p.Val163Met	c.487G>A	A		G/G	91	91,0
MN590	POLL	chr10:103344589	SNV	T	1	T/G	204	106,98	NM_001174084.1	exonic	missense	CCC	p.Thr221Pro	c.661A>C	G		T/T	117	117,0
MN590	PRKDC	chr8:48710955	SNV	A	1	A/G	109	65,44	NM_006904.6	exonic	missense	ACT	p.Ile3433Thr	c.10300T>C	G		A/A	72	72,0
MN590	RAD23B	chr9:110084328	SNV	C	1	C/T	340	68,272	NM_002874.4	exonic	missense	GTT	p.Ala249Val	c.746C>T	T		./.	15	15,0
MN590	RAD54L	chr1:46725684	SNV	G	1	G/A	134	70,64	NM_001142548.1	exonic	missense	CAG	p.Arg107Gln	c.320G>A	A		G/G	76	76,0
MN590	SMUG1	chr12:54577720	SNV	G	1	G/A	146	122,24	NM_001243788.1	exonic	missense	CTC	p.Pro2Leu	c.5C>T	A		G/G	72	72,0
MN590	TOP3B	chr22:22318364	SNV	G	1	G/A	141	62,79	NM_003935.4	exonic	missense	TGG	p.Arg379Trp	c.1135C>T	A		G/G	52	52,0
MN590	XRCC3	chr14:104169515	SNV	C	1	C/A	270	189,81	NM_001100118.1	exonic	missense	TAT	p.Asp186Tyr	c.556G>T	A		C/C	119	120,0

Supplementary methods

In vivo treatment

JQ1 (James Bradner, DFCI/Harvard) was dissolved in DMSO and then diluted with 10% cyclodextran. JQ1 was given at a final dose of 100 mg/kg body weight by i.p. injection once/day. MEK162 was formulated in 1% carboxymethyl cellulose with 0.5% Tween80 and daily delivered orally to mice at 15 mg/kg.

Western blot

Tumor samples were lysed and western blot analysis was performed as previously described[1]. Antibodies against pAKT (S473) (Cell Signaling #4060), AKT (Cell Signaling #9272), HER2 (Calbiochem#OP15), EGFR (Cell Signaling #4267), p110α (Cell Signaling #4249), p110β (Cell Signaling #3011), pMAPK (Cell Signaling #9101), MAPK (Cell Signaling #9102), pS6RP (Cell Signaling #2211), S6RP (Cell Signaling #2217), Vinculin (Sigma#V9131), and α-Tubulin (Sigma#T9026) were applied. Antibody validation is provided by the manufacturers' website.

Reference

1. Ni, J.*, et al.* Functional characterization of an isoform-selective inhibitor of PI3K-p110beta as a potential anticancer agent. *Cancer discovery* **2**, 425-433 (2012).